

Protein disaggregation mediated by heat-shock protein Hsp104

Dawn A. Parsell^{*†‡}, Anthony S. Kowal[†], Mike A. Singer[§] & Susan Lindquist^{*†||}

Departments of ^{*} Molecular Genetics and Cell Biology, [§] Pathology, and [†] The Howard Hughes Medical Institute, The University of Chicago, MC1028 N339, 5841 S. Maryland Avenue, Chicago, Illinois 60637, USA

THE heat-inducible members of the Hsp100 (or Clp) family of proteins share a common function in helping organisms to survive extreme stress, but the basic mechanism through which these proteins function is not understood¹⁻⁵. Hsp104 protects cells against a variety of stresses, under many physiological conditions^{6,7}, and its function has been evolutionarily conserved, at least from *Saccharomyces cerevisiae* to *Arabidopsis thaliana*²⁵. Homology with the *Escherichia coli* ClpA protein suggests that Hsp104 may provide stress tolerance by helping to rid the cell of heat-denatured proteins through proteolysis¹. But genetic analysis indicates that Hsp104 may function like Hsp70 as a molecular chaperone⁸. Here we investigate the role of Hsp104 *in vivo* using a temperature-sensitive *Vibrio harveyi* luciferase-fusion protein as a test substrate⁹. We find that Hsp104 does not protect luciferase from thermal denaturation, nor does it promote proteolysis of luciferase. Rather, Hsp104 functions in a manner not previously described for other heat-shock proteins: it mediates the resolubilization of heat-inactivated luciferase from insoluble aggregates.

We first determined the conditions under which our test substrate would be inactivated while both wild-type and mutant cells remained viable. We found that pretreatment at 37 °C partially protected luciferase from inactivation at extreme temperatures (Fig. 1a) but that luciferase was always inactivated to a comparable extent in wild-type (*HSP104*) and mutant (*hsp104*) cells. We conclude that Hsp104 does not play a significant part in this protection.

To investigate the proposed role of Hsp104 in proteolysis of heat-damaged proteins, we analysed the stability of luciferase after a severe heat shock. Cells were pretreated at 37 °C for 30 min to induce synthesis of heat-shock proteins, shifted to 44 °C for 1 hour, then returned to 25 °C. Cycloheximide was added to block protein synthesis during the recovery period at 25 °C. Luciferase levels remained constant in both wild-type and *hsp104* mutant cells throughout the experiment (Fig. 1b). Thus, Hsp104 does not appear to affect turnover of the heat-inactivated test substrate.

We next investigated whether Hsp104 functions in reactivating heat-damaged proteins. Cells were pretreated at 37 °C, heat-shocked at 44 °C, and then allowed to recover at 25 °C in the absence of new protein synthesis. Wild-type cells recovered 90% of their initial luciferase activity, but *hsp104* mutant cells failed to reactivate the enzyme (Fig. 2a). This result suggests that, rather than serving to rid the cell of stress-damaged proteins, Hsp104 functions to promote their proper renaturation and reactivation. To test the importance of the two ATP-binding sites of Hsp104 for this function, we examined luciferase reactivation in strains expressing *hsp104* alleles containing single inactivating point mutations. As previously demonstrated for thermotolerance², the function of both ATP-binding sites was required for luciferase reactivation (Fig. 2b).

The failure of the *hsp104* strain to reactivate temperature-sensitive bacterial luciferase was reminiscent of the inability of

the *E. coli hsp70 (dnaK)* mutants to restore the activity of denatured firefly luciferase¹⁰. To investigate the role of yeast Hsp70 proteins in reactivation, we examined mutants in which Hsp70 levels were diminished either by reducing constitutive expression (*ssa1ssa2*) or eliminating heat-inducible expression (*ssa1ssa3ssa4*). The basal level of luciferase activity was reduced approximately fourfold in the *ssa1ssa2* strain. In both of the *hsp70* mutant strains, the enzyme was inactivated by heat shock at 44 °C to roughly the same extent as in the wild type. In contrast to the *hsp104* mutant, however, the *ssa1ssa3ssa4* mutant recovered luciferase activity at 25 °C as efficiently as the wild type. The *ssa1ssa2* mutant also recovered substantially (Fig. 2c). Only when Hsp104 was eliminated in the *hsp70* mutant background were cells unable to reactivate luciferase.

To investigate the state of the test substrate in wild-type, *hsp70*, and *hsp104* mutant cells, lysates were prepared at various times during the luciferase inactivation/reactivation experiment. These lysates were centrifuged at high speed and the fraction of luciferase remaining in the supernatant determined. Heat inactivation gave a dramatic decrease in the concentration of soluble luciferase in all cell types (Fig. 3). In wild-type and *hsp70* mutant

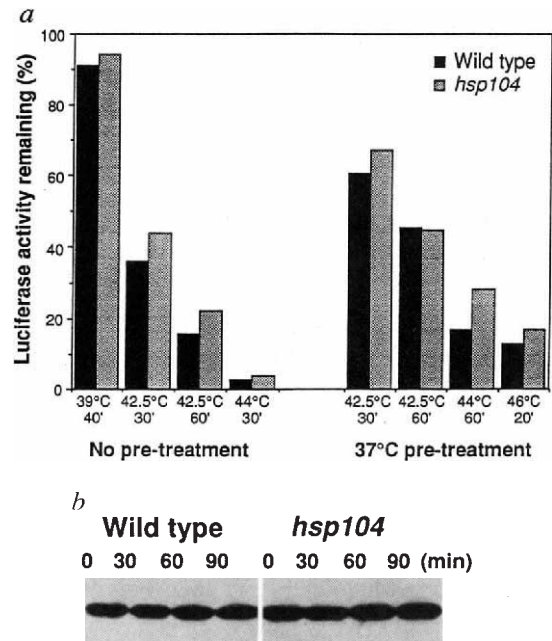


FIG. 1 a, Heat inactivation of luciferase in wild-type and *hsp104* mutant yeast cells. Wild-type (strain A1456) and *hsp104* mutant (strain A1458) cells, bearing 2 μ plasmids that direct the expression of a temperature-sensitive luciferase-fusion protein⁹ from the constitutive glyceroldehydro-3-phosphate dehydrogenase promoter (pGPDluxAB(HIS)), were grown at 25 °C to mid-log phase in minimal dextrose medium¹⁹ supplemented with nutrients. Cultures were shifted to high temperature for the indicated lengths of time either with (right) or without (left) a preconditioning treatment of 37 °C for 30 min. Luciferase activity was assayed *in vivo* by adding 10 μ l of *n*-decylaldehyde (Sigma) to 1 ml log-phase cultures. Light emission was measured immediately with a Tropic luminometer. Activity levels are expressed as a percentage of the activity before the heat treatment. All strains are derivatives of W303 (gift from R. J. Rothstein). b, Luciferase protein levels do not change during heat inactivation and recovery. Wild-type and *hsp104* mutant cells bearing the luciferase expression plasmid were grown at 25 °C, pretreated at 37 °C for 30 min to induce Hsp expression, shifted to 44 °C for 60 min to inactivate luciferase and then allowed to recover at 25 °C. Cycloheximide (10 μ g ml⁻¹) was added during the last 10 min of the 44 °C treatment to block further protein synthesis. Total cellular proteins were extracted from cells at intervals during recovery using glass-bead lysis²⁰ and separated by SDS-PAGE on 10% gels²¹, transferred to Immobilon membranes (Millipore) and reacted with luciferase-specific antiserum. Immune complexes were visualized using horseradish-peroxidase-conjugated protein A and ECL detection system (Amersham).

[‡] Present address: Connective Therapeutics Inc., 3400 West Bayshore Road, Palo Alto, California 94303, USA.

^{||} To whom correspondence should be addressed.

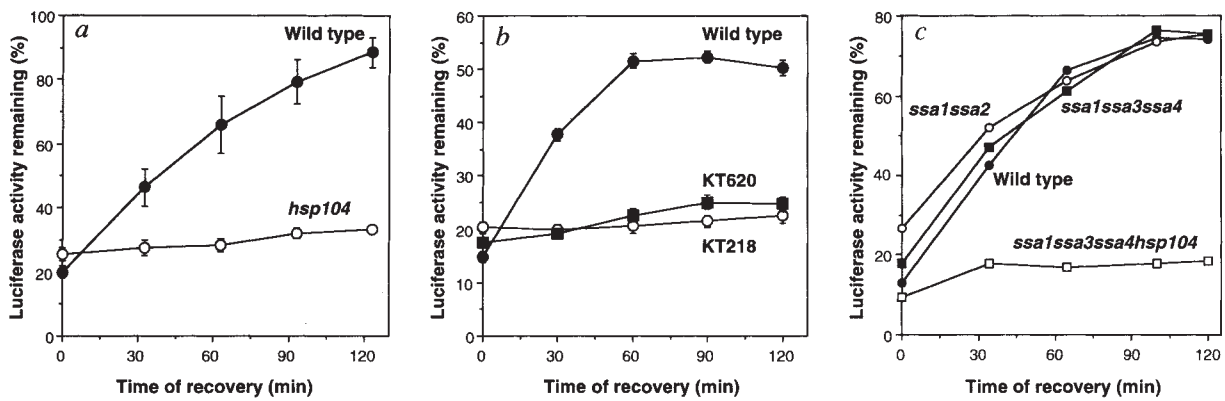


FIG. 2 Reactivation of heat-damaged luciferase requires Hsp104. *a*, Wild-type (filled circles) and *hsp104* mutant (circles) cells bearing the luciferase expression plasmid were treated as described for Fig. 1*b* and luciferase activity assayed *in vivo* as in Fig. 1*a*. Activity, expressed as a percentage of the luciferase activity in cells just before the 44 °C heat shock, was measured in duplicate for each of three separate cultures for each strain. *b*, *hsp104* mutant cells carrying the luciferase expression construct and a centromeric plasmid encoding either the wild-type HSP104 gene (filled circles; strain A1625) or an *hsp104* allele containing a mutation (lysine to threonine) which destroys the function of the

first (circles; strain A1626) or second (filled squares; strain A1627) ATP-binding site of the protein, were assayed for luciferase activity. Expression of all three alleles was driven by the HSP104 promoter. *c*, *S. cerevisiae* strains^{8,22} carrying mutations in the heat-inducible (filled squares; strain A1592: *ssa1ssa3ssa4*) or constitutive (circles; strain A1591: *ssa1ssa2*) cytosolic/nuclear *hsp70* genes were assayed for luciferase activity. For comparison, luciferase reactivation was measured in a wild-type strain (filled circles; strain A1630) and in a strain carrying mutation in both the heat-inducible Hsp70 genes and in Hsp104 (squares; A1593: *ssa1ssa3ssa4 hsp104*).

cells, luciferase was resolubilized during the course of recovery at 25 °C but there was little resolubilization of luciferase in *hsp104* mutant cells. Thus, it appears that Hsp104 promotes the restoration of luciferase activity by facilitating resolubilization of this protein from insoluble aggregates.

To determine whether the function of Hsp104 in promoting the resolubilization of luciferase reflects its general role in stress tolerance, cells were examined by electron microscopy. Wild-type and mutant cells that did not contain luciferase-expressing plasmids were subjected to the conditions used for the luciferase inactivation/reactivation experiments. The morphology of both wild-type and *hsp104* cells was normal at 25 °C (Fig. 4*a*). After heat treatment at 44 °C, damage was evidenced by the accumulation of large electron-dense aggregates in the cytoplasm and, more dramatically, in the nucleus. The severity of this damage was indistinguishable in the two cell types. In wild-type cells, this damage was resolved during recovery at 25 °C. After 120 min at 25 °C, damage had disappeared from almost all wild-type cells (Fig. 4*a, b*). Although *hsp70* strains continued to show abnormalities, particularly in membrane structures (A.S.K. and S.L.,

unpublished), after 120 min of recovery at 25 °C aggregation damage was resolved almost as well as in wild-type cells (Fig. 4*c*).

In contrast, *hsp104* mutant cells did not resolve the aggregation damage generated by heat treatment at 44 °C. Even after 120 min of recovery, most *hsp104* cells were still almost as damaged as they were immediately after heat shock (Fig. 4*a, b*). The aggregates seen here are not simply a consequence of cell death as both wild-type and *hsp104* mutant cells are viable under these conditions (data not shown). We believe, however, that these aggregates are directly related to the primary lethal lesion caused by treatment at higher temperatures, because similar aggregates are observed in wild-type cells at lethal temperatures¹¹.

In summary, we have shown that Hsp104 functions to reactivate a heat-denatured protein by promoting its resolubilization from an aggregated form. Ultrastructural analysis of heat-shocked cells indicates that this reactivation function is broad and represents the mechanism by which Hsp104 promotes survival under extreme stress. Our findings also help to distinguish the roles of Hsp70 and Hsp104 in thermotolerance. Strains lack-

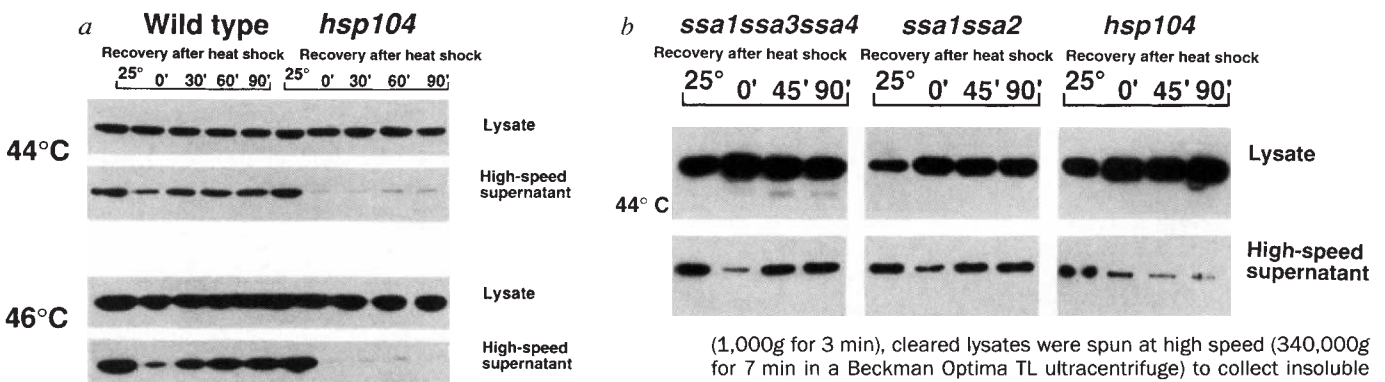


FIG. 3 Hsp104 promotes the resolubilization of aggregated luciferase. *a*, Wild-type and *hsp104* mutant cells carrying the luciferase expression plasmid were pretreated at 37 °C for 30 min, heat-shocked at either 44 °C for 60 min or at 46 °C for 24 min, then allowed to recover at 25 °C after adding cycloheximide and lysed as for Fig. 1 using glass-bead lysis. After removing unbroken cells by low-speed centrifugation

(1,000g for 3 min), cleared lysates were spun at high speed (340,000g for 7 min in a Beckman Optima TL ultracentrifuge) to collect insoluble aggregates. Total protein from the cleared lysates and high-speed supernatants was western blotted and probed as described in Fig. 1 legend. *b*, *ssa1ssa3ssa4* and *ssa1ssa2* mutants were treated as in *a*, with heat shock at 44 °C for 60 min. Coomassie staining of the blot demonstrated equal loading of all but the 25 °C samples, which were underloaded (data not shown). Because *ssa1ssa2* strains contained less luciferase, exposure was longer for these samples.

FIG. 4 *hsp104* mutants are unable to resolve heat-induced aggregates that are visible by electron microscopy. *a*, Wild-type and *hsp104* mutant cells were grown at 25 °C to mid-log phase in rich dextrose medium¹⁹. Cells were pretreated, heat-shocked at 44 °C for 60 min, and allowed to recover as in Fig. 3. Portions of the cultures were collected before any heat treatment (25 °C), immediately after the 44 °C heat shock (0 min), after 45 min of recovery at 25 °C (45 min) and after 120 min of recovery at 25 °C (120 min). *b*, For each of the samples in *a*, electron micrograph fields of 52–100 cells were screened (double blind) for aggregated material at 25 °C before heat treatment, immediately after 44 °C treatment (0'), after 45 min of recovery at 25 °C (45'), and after 120 min of recovery at 25 °C (120'). *c*, Wild-type, *ssa1ssa2* and *ssa1ssa3ssa4* cells were prepared as for *a* and electron micrograph fields of 31–151 cells evaluated for aggregated material as for *b*.

METHODS. Cells were fixed overnight at 4 °C in 40 mM potassium phosphate (pH 6.8) containing 1 mM MgCl₂, 1% glutaraldehyde and 1% paraformaldehyde^{22,23}. After washing, cells were incubated for 15 min at room temperature in 1% sodium metaperiodate, washed, resuspended in 50 mM ammonium chloride for 30 min²⁴, washed, and post-fixed for 60 min in 2% osmium tetroxide in buffer containing 40 mM potassium phosphate (pH 6.8) 1 mM MgCl₂. Cells were washed with water, then stained overnight at 4 °C with 0.5% uranyl acetate²² in 40 mM sodium malate (pH 5.2), washed, dehydrated with ethanol, and washed three times with 100% propylene oxide, then gradually infiltrated with resin.

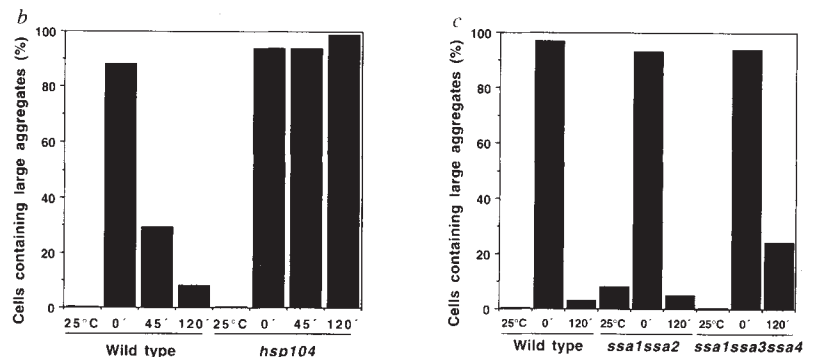
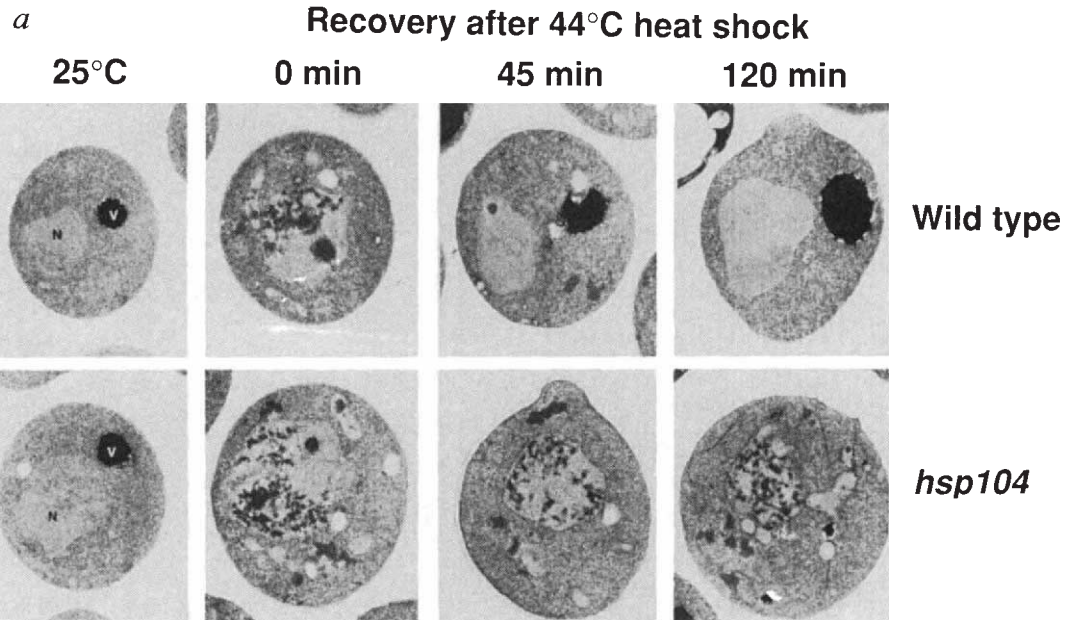
ing either the constitutive or the heat-inducible Hsp70 proteins recover luciferase activity almost to wild-type levels and resolve general aggregation damage nearly as well as wild-type cells. Although these results are surprising, given that *dnaK* mutants are unable to reactivate heat-denatured firefly luciferase in *E. coli*, they agree with the properties of DnaK *in vitro*¹⁰. DnaK can only reactivate firefly luciferase if luciferase has been prevented, by DnaJ, from aggregating. Under our conditions, heat-denatured proteins could presumably not be reactivated by Hsp70 because they were already aggregated (Figs 3, 4). A disaggregation activity has been reported for DnaK with an RNA polymerase substrate¹², but as core polymerase forms oligomers under such conditions¹³, this activity could reflect the ability of DnaK to disassemble certain types of protein oligomers^{13,15}. Although Hsp70 may promote the dissolution of some protein aggregates, we suggest that its primary function in thermotolerance is to help prevent such aggregates from forming^{10,12,16}. Hsp104, in contrast, has a remarkable capacity to rescue proteins from aggregates once they have formed. Hsp70 and Hsp104 can partially compensate for one another⁸ because they both affect the partitioning of damaged substrates between a denatured, soluble state and an insoluble, aggregated one. Thus, although their biochemical activities are distinct, both proteins function along the same general pathway.

Complementarity in the functions of Hsp104 and Hsp70 helps to explain why different species depend on different constellations of heat-shock proteins for thermotolerance¹⁷. *Drosophila*,

for example, does not even express an Hsp100 protein in response to heat; instead, it relies upon massive synthesis of Hsp70 directed by amplified genes (see ref. 17 for review). All organisms must: (1) balance the beneficial functions of particular heat-shock proteins against their detrimental effects^{8,18}; (2) use the heat-shock proteins that are most effective in protecting or repairing their own most critical cellular targets; and (3) develop a response appropriate for the types of stress they normally encounter. Thus, stress responses represent a balance between the biochemical advantages and disadvantages of the various heat-shock proteins within the context of a particular physiology and environment. □

Received 30 August; accepted 17 October 1994.

- Gottesman, S. *et al.* *Proc. natn. Acad. Sci. U.S.A.* **87**, 3513–3517 (1990).
- Parsell, D. A., Sanchez, Y., Stitzel, J. D. & Lindquist, S. *Nature* **353**, 270–273 (1991).
- Squires, C. L., Pedersen, S., Ross, B. M. & Squires, C. J. *Bact.* **173**, 4254–4262 (1991).
- Squires, C. & Squires, C. L. *J. Bact.* **174**, 1081–1085 (1992).
- Kruger, E., Volker, U. & Hecker, M. *J. Bact.* **176**, 3360–3367 (1994).
- Sanchez, Y., Taulien, J., Borkovich, K. A. & Lindquist, S. *EMBO J.* **11**, 2357–2364 (1992).
- Sanchez, Y. & Lindquist, S. L. *Science* **248**, 1112–1115 (1990).
- Sanchez, Y. *et al.* *J. Bact.* **175**, 6484–6491 (1993).
- Escher, A., O'Kane, D. J., Lee, J. & Szalay, A. A. *Proc. natn. Acad. Sci. U.S.A.* **86**, 6528–6532 (1989).
- Schroder, H. T., Langer, T., Hartl, F.-U. & Bukau, B. *EMBO J.* **12**, 4137–4144 (1993).
- Webster, D. L. & Watson, K. *Yeast* **9**, 1165–1175 (1993).
- Skowyra, D., Georgopoulos, C. & Zyllic, M. *Cell* **62**, 939–944 (1990).
- Shanen, S. L. *et al.* *Biochemistry* **21**, 5539–5551 (1982).
- Wickner, S., Hoskins, J. & McKenney, K. *Nature* **350**, 165–167 (1991).
- Wickner, S., Hoskins, J. & McKenney, K. *Proc. natn. Acad. Sci. U.S.A.* **88**, 7903–7907 (1991).



Sections were stained with 4% aqueous uranyl acetate, washed, stained with 0.2% lead citrate, and viewed with a Phillips CM10 transmission electron microscope at 60 kV. Magnification, $\times 7,440$.

16. Langer, T. *et al.* *Nature* **356**, 683–689 (1992).
 17. Parsell, D. A. & Lindquist, S. *A. Rev. Genet.* **27**, 437–496 (1993).
 18. Feder, J. J., Rossi, J. M., Solomon, J., Solomon, N. & Lindquist, S. *Genes Dev.* **6**, 1402–1413 (1992).
 19. Treco, D. A. in *Current Protocols in Molecular Biology* (eds Ausubel, F. M., Brent, R. & Kingston, R. E.) 13.1.1–13.1.7 (Wiley, New York, 1989).
 20. Kurtz, S., Gordon, E. & Lindquist, S. L. in *Sequence Specificity in Transcription and Translation* 611–620 (Liss, New York, 1985).
 21. Laemmli, U. K. *Nature* **227**, 680–685 (1970).
 22. Wright, R. & Rine, J. in *Methods in Cell Biology* (ed. Tartakoff, A. M.) 473–512 (Academic, New York, 1989).
 23. Byers, B. & Goetsch, L. *Meth. Enzym.* **194**, 602–608 (1991).
 24. van Tuinen, E. & Riezman, H. J. *Histochem. Cytochem.* **35**, 327–333 (1987).
 25. Schirmer, E., Lindquist, S. & Vierling, E. *Pl. Cell* (in the press).

ACKNOWLEDGEMENTS. We thank A. Szalay and A. Escher for the luciferase fusion gene and for luciferase-specific antiserum. Y. Sanchez, together with A.S.K. and S.L., made the original observation of aggregates in *hsp104* mutant cells. We thank E. Schirmer and J. Vogel for critical reading of the manuscript, and D. Wang for assistance in preparing figures.

The X-ray structure of a growth hormone–prolactin receptor complex

William Somers, Mark Utsch, Abraham M. De Vos & Anthony A. Kossiakoff*

Genentech Inc., Department of Protein Engineering,
 460 Point San Bruno Boulevard, South San Francisco,
 California 94080, USA

THE human pituitary hormones, growth hormone (hGH) and prolactin (hPRL), regulate a large variety of physiological processes, among which are growth and differentiation of muscle, bone and cartilage cells, and lactation¹. These activities are initiated by hormone–receptor binding. The hGH and hPRL receptors (hGH_R and hPRL_R, respectively) are single-pass transmembrane receptors from class I of the haematopoietic receptor superfamily^{2,3}. This classification is based on sequence similarity in their extracellular domains, notably a highly conserved pentapeptide, the so-called ‘WSXWS box’, the function of which is controversial. All ligands in class I activate their respective receptors by clustering mechanisms⁴. In the case of hGH, activation involves receptor homodimerization in a sequential process: the active ternary complex containing one ligand and two receptor molecules is formed by association of a receptor molecule to an intermediate 1:1 complex^{5–8}. hPRL does not bind to the hGH receptor, but hGH binds to both the hGH_R and hPRL_R, and mutagenesis studies have shown that the receptor-binding sites on hGH overlap⁹. We present here the crystal structure of the 1:1 complex of hGH bound to the extracellular domain of the hPRL_R. Comparisons with the hGH–hGH_R complex¹⁰ reveal how hGH can bind to the two distinctly different receptor binding surfaces.

As the extracellular domain of the hPRL_R only forms a stable 1:1 complex with hGH in solution, we used this complex in our crystallographic studies. The structure of this complex (Fig. 1a) was determined at 2.9 Å resolution and refined to a crystallographic *R*-factor of 0.22 (Table 1). The overall similarity with the hGH–hGH_R complex¹⁰ (Fig. 1b) can be seen in Fig. 1c, which shows the superposition of the structure of the hGH–hPRL_R complex on the equivalent 1:1 portion of the 1:2 hGH–hGH_R complex. The hGH molecule has the classical cytokine fold⁴, a four-helix bundle motif characterized by the first two helices running parallel to each other but antiparallel to the last two. The four-helix bundle structure of the hGH molecule in the hPRL_R complex superimposes well on that of the hGH_R (1:2) complex (0.82 Å r.m.s. on *Ca* positions). Larger

TABLE 1 Crystallographic data, refinement statistics and interfacial hydrogen bonds

Data collection statistics				
Dataset	Number of crystals	Number of observations	Number of reflections	<i>R</i> _{merge}
FAST	3	35,239	9,754	0.077
SSRL	6	17,794	8,293	0.095
Combined	9	53,033	9,883	0.108
Refinement statistics				
No. non-hydrogen atoms	3,123			
Disordered residues	hGH: 149–152, 191; hPRL _R : 1, 31–33, 84–86, 205–211			
Average <i>B</i> -factor	hGH: 55 Å ² ; hPRL _R : 42 Å ²			
Resolution range	10–2.9 Å			
<i>R</i> -value (all data)	0.22			
r.m.s. bond length deviation	0.019 Å			
r.m.s. bond angle distance deviation	0.046 Å			
r.m.s. difference in <i>B</i> -factor	0.63 Å ² (main chain atoms), 0.66 Å ² (side-chain atoms)			
Intermolecular hydrogen bonds in hGH–hPRL _R and hGH–hGH _R				
hGH	hPRL _R	hGH	hGH _R	
Ser 62 O	Met 103 N	Pro 61 O	Ile 103 N	
Lys 168 Nζ	Trp 104 O	Lys 168 Nζ	Trp 104 O	
Ser 51 Oγ	Glu 75 Oε2	Lys 41 Nζ	Glu 127 Oε2	
Tyr 164 Oη	Glu 75 Oε1	Arg 167 Nη1	Glu 127 Oε1	
Arg 167 Nη2	Asp 124 Oδ2	Arg 167 Nη2	Glu 127 Oε1	
Arg 178 Nη1	Thr 171 Oγ1	Arg 178 Nη2	Ile 165 O	
Arg 178 Nη1	Phe 170 O	Thr 175 Oγ1	Arg 43 Nη1	
Arg 178 Nη2	Gln 193 Oε2	Gln 46 Nε2	Glu 120 Oε2	
Asp 171 Oδ1	Tyr 127 Oη	Asp 171 Oδ2	Arg 43 Nη2	

hGH and hPRL_R were purified, complexed and crystallized as described¹⁶. Crystals were in space group *P*₂₁₂₁₂, with *a* = 154.2 Å, *b* = 69.8 Å, *c* = 43.4 Å. Data were collected at room temperature from three crystals using an Enraf-Nonius FAST area detector mounted on a Rigaku RU200 rotating anode generator and monochromated CuKα X-rays, and processed using MADNES¹⁷ and PROCOR¹⁸. The program X-PLOR¹⁹ was used for molecular replacement with the 1:1 hGH–hGH_R structure (A.M.d.V., unpublished results) as a search model. The rotation function gave no clear solutions, but Patterson correlation (PC) refinement²⁰ of the rotation function peaks treating the hormone and both receptor domains as independent rigid bodies gave a solution with a PC value of 0.13, clearly above the highest noise peak at 0.07 (data between 15 and 4 Å resolution). The translation search gave a correlation value of 0.36 with the highest noise peak at 0.24 and a crystallographic *R*-value of 0.49, decreased to 0.47 by rigid-body refinement (15–3.5 Å). The refinement dataset was generated by merging the molecular replacement dataset with data collected at the Stanford Synchrotron Radiation Laboratory (SSRL) on a MAR image plate scanner and processed with XDS¹⁸, giving an overall completeness of 93% (89% between 3 and 2.9 Å). The structure was refined using a combination of simulated annealing and positional refinement with X-PLOR and manual intervention using FRODO²¹. The final stages of refinement were performed using PROLSQ²² with highly-restrained individual temperature factors, resulting in an *R*-value of 0.22 (10–2.9 Å).

differences are found in the loop structures and in two small mini-helices. The loop connecting helices 2 and 3 (residues 92–111) does not contact the receptor and generally is not well ordered. The first turn in helix 3 is partially unwound compared to the structure of the hGH–hGH_R complex; a similar unwinding occurs in the structure of a free hGH variant¹¹. The loop connecting helices 3 and 4 is also poorly ordered, but was modelled into weak electron density in a similar conformation as observed in the 1:1 hGH_R complex. The complexes also differ at mini-helix 1 (M1 in Fig. 1, residues 42–46), in which the N-terminal turn is partially unwound, and in the segment of loop immediately following it. Because changes in this region have also been seen in the structure of the hGH variant, where it

* To whom correspondence should be addressed.